

# Vortex Dynamics in an Annular Bose-Einstein Condensate

S. J. Woo\* and Young-Woo Son†

*Korea Institute for Advanced Study, Seoul 130-722, Korea*

(Dated: March 8, 2013)

We theoretically show that the topology of a non-simply-connected annular atomic Bose-Einstein condensate enforces the inner surface waves to be always excited with outer surface excitations and that the inner surface modes are associated with induced vortex dipoles unlike the surface waves of a simply-connected one with vortex monopoles. Consequently, under stirring to drive an inner surface wave, a peculiar population oscillation between the inner and outer surface is generated regardless of annulus thickness. Moreover, a new vortex nucleation process by stirring is observed that can merge the inner vortex dipoles and outer vortex into a single vortex inside the annulus. The energy spectrum for a rotating annular condensate with a vortex at the center also reveals the distinct connection of the Tkachenko modes of a vortex lattice to its inner surface excitations.

PACS numbers: 03.75.Kk, 03.75.Lm, 67.85.De

An atomic Bose-Einstein condensate (BEC) has been considered as an excellent many-body macroscopic quantum system with experimentally controllable parameters such as number density, inter-particle interaction, spin, confining potential and so on. Recently, topology of BEC also becomes to be important as in many different fields of physics. For example, the realization of a circular waveguide for an atomic BEC [1, 2] was followed by the achievement of a topologically non-simply-connected atomic condensate in a magnetic toroidal trap with a plug laser. It shows the first observation of atomic superfluid persistent current [3] which was further refined to stay longer than 40 seconds in an all optical trap [4].

In torus BECs, there have been many interesting phenomena related with topological aspect: vortex lattice formation [5, 6], dynamics of vortices and solitons under stirring [7–10], and dynamics of vortex dipoles [10–12]. In order to understand the formation and decay of vortices in a superfluid related with the toroidal persistent current, the knowledge of low-lying energy spectrum and dynamics is essential. When the torus BEC has flat shape with strong confinement along one direction, a toroidal condensate has two distinguishable surfaces, inner and outer surfaces (called as an annular BEC hereafter). The normal mode spectrum calculations for such an annular BEC available currently, however, have been done only within quasi-1D regime where the azimuthal degree of freedom is meaningful [13], while in the experiments radial degree of freedom cannot be ignored [3, 4].

In this Letter, we calculate numerically the normal mode dynamics of an annular BEC within mean field regime considering the azimuthal and radial degrees of freedom fully compatible with current experiments [3, 4]. We have found that the excitations on the inner surface of a non-rotating annular BEC are associated with vortex dipoles rather than monopoles and that such in-

ner surface excitations cannot be excited by themselves. Those aspects suggest topologically distinct phenomena of annular BECs when they are stirred, e.g., population oscillations between inner and outer surfaces and topological excitations by vortex dipoles. A rotating annular BEC with nontrivial angular momentum is achieved by imposing quantized vorticity that penetrates the hollow region of the annulus. It is also found that such penetrating vortices, which would give vortex lattice excitations, Tkachenko modes, if they were in a simply-connected BEC, play a crucial role in determining the inner surface excitations of a rotating annular condensate.

To describe the normal mode excitations, we solve Bogoliubov-de Gennes equations [14, 15] numerically using finite element technique with Hermite polynomial basis [18];  $\mathcal{L}u_j - g\psi_0^2 v_j = \hbar\omega_j u_j$  and  $\mathcal{L}v_j - g\psi_0^{*2} u_j = -\hbar\omega_j v_j$  where  $\mathcal{L} = -\frac{\hbar^2 \nabla^2}{2M} + V_{\text{tr}}(\mathbf{r}) + 2g|\psi_0|^2 - \mu$ . The toroidal trap potential is  $V_{\text{tr}} = \frac{M}{2}(\omega_{xy}^2(r - r_0)^2 + \omega_z^2 z^2)$  where  $r = (x^2 + y^2)^{1/2}$  as shown in Fig. 1(a). Interparticle coupling constant is  $g = \frac{4\pi a \hbar^2}{M}$  with the  $s$ -wave scattering length  $a$ ,  $\mu$  the chemical potential and  $\psi_0$  the ground state wave function of the condensate.  $u_j$ ,  $v_j$ , and  $\omega_j$  represent the wave functions and eigenenergy for the  $j$ -th quasiparticle excitation, respectively.  $\psi_0$  and  $\mu$  are determined by solving time-independent Gross-Pitaevskii equation (GPE),  $(-\frac{\hbar^2 \nabla^2}{2M} + V_{\text{tr}}(\mathbf{r}) + g|\psi_0|^2 - \mu)\psi_0 = 0$  where  $\psi_0$  is normalized by the total number of particles,  $N = \int d\mathbf{r} |\psi_0|^2$ . Strong confinement along the  $z$ -axis,  $\omega_{xy} \ll \omega_z$ , is assumed. All values here are based on the dimension of the trap potential [16]. Fig. 1 (b) is the den-

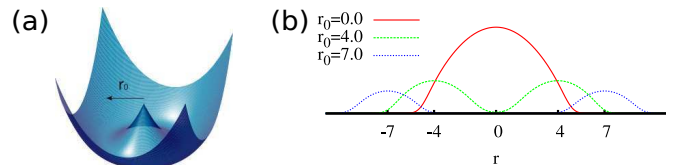


FIG. 1: (Color online) (a) Torus trapping potential. (b) The radial density distribution of BEC for various torus radii.

\*Electronic address: sjwoo@kias.re.kr

†Electronic address: hand@kias.re.kr

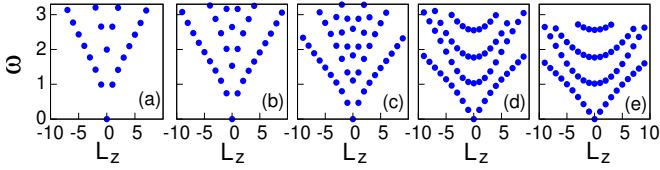


FIG. 2: (Color online) Angular momentum ( $L_z$ ) vs. energy ( $\omega$ ) curves for different  $r_0$  values for a non-rotating condensate:  $r_0 = 0$  (a), 2 (b), 4 (c), 6 (d) and 7 (e).

sity of condensate along the radial direction for  $N = 5000$  and  $g = 0.1$  for different  $r_0$  values.

Normal mode dynamics can be visualized by noting that  $\psi_j(t) = \psi_0 + \sqrt{n_q}(u_j e^{-i\omega_j} - v_j^* e^{i\omega_j})$  satisfies time-dependent GPE [14, 15]. Fig. 2 shows the energy vs. angular momentum dispersion relations of a BEC for different  $r_0$  values: (a)  $r_0 = 0$  and (b)  $r_0 = 2$  correspond to simply-connected BECs, (c)  $r_0 = 4$  for the transition region, and (d) and (e) ( $r_0 > 4$ ) are for annulus cases. We categorize the normal modes using a pair of the radial ( $n$ ) and angular ( $m$ ) quantum numbers, i.e.,  $(n, m)$  mode, as in a simply-connected case;  $n$  and  $m$  represent the number of nodes along the radial and angular direction respectively [17]. Here we notice that the energy dispersion curves as functions of  $m$  for either simply connected or annular condensate show well separated classes of normal modes with quantum number  $n$ 's.

First, we have found that the surface waves with the lowest radial quantum number ( $n = 0$ ) cannot be generated along the inner surface of an annulus even though an additional surface forms on its inner side. As  $r_0$  changes from 0 to 7 crossing the critical point at  $r_0 \approx 4$ , every normal mode can adiabatically be transformed. The modes in the lowest curve ( $n = 0$ ) in Figs. 2 (d) or (e) correspond to normal modes with longitudinal density wave propagating along the radial direction. Especially with higher  $|m|$ ,  $n = 0$  density waves appear mainly as surface waves mostly on the outer surface as in the simply-connected case [17]; Fig. 3 (a) shows the contour plot of a snapshot for the density of  $(0, 14)$  normal mode. Fig. 3 (d) represents the inner and outer edges if the annulus were to be unwound with the corresponding induced vortex singularity positions. Another schematic plot, Fig. 3 (g), shows two density plots along the radial direction at two different angular positions  $A$  and  $B$  in Fig. 3 (a) which shows the density fluctuation at a certain fixed angular position.

Next, we show that, unlike the case for the lowest radial mode ( $n = 0$ ), both inner and outer surfaces host surface wave excitations for higher radial modes. In Fig. 2 (d) or (e), the next lowest curve ( $n = 1$ ) corresponds to out-of-phase surface excitations with both inner and outer surface waves, of which wave nodes are placed alternatively along the angular direction. The corresponding modes in a simply-connected case, Fig. 2 (a) or (b), are those with one radial node including breathing mode [17]. The  $(1, 0)$  breathing mode in a simply-connected case has the well-

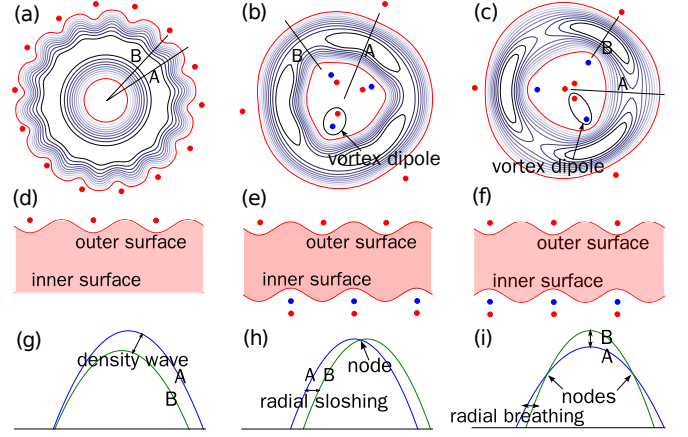


FIG. 3: (Color online) Contours for snapshots of  $|\psi_j(t)|^2$  for modes with  $(n, m) =$  (a)  $(0, 14)$  (b)  $(1, 3)$  and (c)  $(2, 3)$ . Darker blue contour lines represent higher densities while red lines are drawn to clarify the density edges. Red (blue) dots represent induced (anti)vortices associated with the excited normal modes propagating counterclockwise and clarify where the wave nodes are. Contours (a), (b), and (c) are schematically unwound in (d), (e) and (f) with vortex singularities propagating leftwards, respectively. Cross sectional density fluctuations along the lines  $A$  and  $B$  in (a), (b), and (c) are schematically drawn in (g), (h) and (i), respectively.

known many-body breathing frequency  $2\omega_{xy}$  [19]. One can see that such a breathing mode would transform into a radial sloshing mode centered at  $r = r_0$  as the condensate gets annular-shaped and hence the frequency becomes corresponding radial trap frequency,  $\omega_{xy}$ .

Figure 3 (b) shows the snapshot of  $(1, 3)$  mode. It should be emphasized that the inner surface wave is accompanied by vortex-antivortex pairs, *vortex dipoles*, differently from the outer surface wave that is accompanied by induced vortices or antivortices depending on the direction of the wave. The critical difference between the two surface waves is that the associated vortex singularities for an inner surface wave are enclosed by the annulus of condensate while those for an outer one are not. Due to this, the induced vorticities on the inner surface will inevitably generate supercurrent, a topological excitation, while those on the outer surface do not. By introducing a vortex dipole inside the annular BEC the vortex or antivortex whichever is closer to the inner surface makes a propagating node in the surface wave while the other can annihilate the generated supercurrent. This property, which is a key finding in this work, is attributed to the topological aspect of annular geometry and the vortex excitations. A schematic plot, Fig. 3 (e), shows that an out-of-phase surface wave is in fact a transverse density wave. Furthermore, Fig. 3 (h) clarifies that the number of radial nodes ( $n$ ) should be one for this specific radial center-of-mass dynamics, i.e., radial sloshing.

The third curve ( $n = 2$ ) in Fig. 2 (d) or (e) corresponds to in-phase excitations with both inner and outer surface waves, of which wave nodes are placed at the

same angular positions. The corresponding modes in a simply-connected case, Fig. 2 (a), are modes with two radial nodes [17]. As  $r_0$  increases, modes with  $n = 2$  make radial breathing dynamics centered at  $r = r_0$  so that the frequency converges to near  $2\omega_{xy}$  for  $m = 0$ . The (2,3) mode [Fig. 3 (c)] also shows vortex dipoles for the inner surface excitation. Figure 3 (f) is a schematic plot showing more clearly that an in-phase surface wave is a longitudinal density wave while Fig. 3 (i) shows that the number of radial nodes is two. In general, modes with higher  $n$  show similar surface waves, in-phase for even  $n$ 's and out-of-phase for odd  $n$ 's while they have additional radial nodes.

Having categorized all the normal modes, it is noted that an inner surface wave should always be excited with an outer surface wave, either in-phase or out-of-phase. This implies that, if one drives an inner surface wave by stirring, it will not stay steady. It is rather a combination of different in-phase and out-of-phase states which will generate beating, hence showing population oscillation with outer-surface wave independent of the annulus thickness. In order to confirm this, we use a modified trap potential mimicking inner surface mode such as  $V_\epsilon = V_{tr}(1 + \epsilon \cos(k\theta))$  when  $r < r_0$  and otherwise  $V_\epsilon = V_{tr}$  ( $k$  is a non-zero integer). We obtain the ground state  $\psi_\epsilon$  for  $V_\epsilon$  that has an inner surface density modulation. Then let it evolve in time in  $V_{tr}$  after turning off  $\epsilon$  to be zero. Our simulation for an annular BEC of  $r_0 = 7$  shows that the inner surface density modulation propagates through the annulus reaching the outer surface and then back onto the inner, making a population oscillation

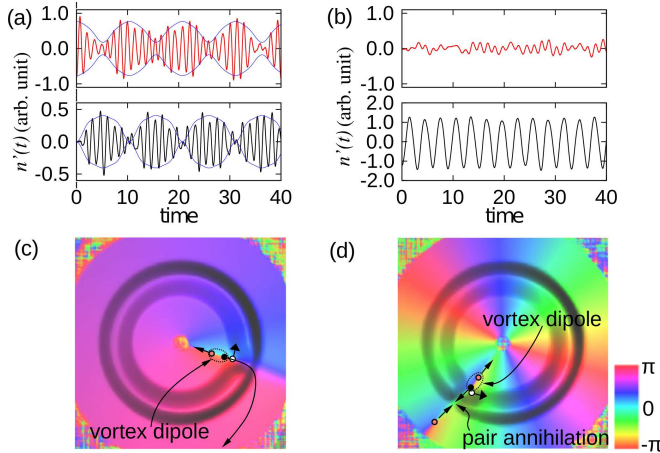


FIG. 4: (Color online) The density fluctuation ( $n'(t) = \psi(t)^2 - \psi_0^2$  [17]) of the inner (red) and outer (black) surface at  $\theta = 0$  as a function of time when either only (a) the inner or (b) outer is excited at  $t = 0$ . Thin blue lines in (a) are guides for eyes. Snapshot of  $\psi(t) = \sqrt{\rho}e^{i\phi}$  under gaussian stirrer (white dot) with slow (c) and fast (d) speed. The height of the surface represents  $\sqrt{\rho}$  while the color  $\phi$ . Red (black) circles represent (anti)vortices around which  $\phi$  has  $\pm 2\pi$  winding. The black arrows in (c) and (d) denote the motions of vortices.

between the two surface waves [Fig. 4 (a)]. On the other hand, we have also confirmed that an initial density modulation on the outer surface makes a density fluctuation only there without any penetration at all [Fig. 4 (b)].

Another peculiar topological feature is in the nucleation process of vortices that can introduce a net topological winding number within the annulus. As shown in Fig. 3(c), the annulus has a vortex-antivortex pair inside while a vortex outside along the same angular position. If the annulus is stirred for inner and outer excitations to merge, they will annihilate themselves leaving a vortex inside the annulus, a topological excitation. Such vortex nucleation procedure cannot occur in a simply-connected case where phase singularities are typically generated outside and then get into the condensate via surface excitations. In order to confirm this scenario, we have simulated stirring an annular BEC ( $r_0 = 10$ ) with a narrow gaussian stirrer on the inner surface. Initially, the ground state is obtained with a gaussian stirrer fixed on the inner edge and then the speed of the stirrer is ramped up along the inner surface adiabatically at the angular acceleration of  $10^{-5}\omega_{xy}^2/\pi^2$ . Figure 4 (c) shows the emergence of the first vortex dipole inside the annulus followed by the decay of the antivortex part of the dipole through the density dip near the stirrer leaving a vortex within the annulus generating supercurrent. Figure 4 (d) shows a similar case with two vortices already within the annulus at higher stirrer speed; a vortex dipole inside the annulus emerges together with a vortex outside followed by pair annihilation of the antivortex part of the dipole and the vortex outside on the rim of the annulus adding another vortex within the annulus.

Now, let us look into the dynamics of an annular BEC with perpetual supercurrent; how the low-lying dynamics is affected by the current-carrying vortex at the torus center. Our calculations have been done in the lab frame. Figure 5 is the rotating-case counterpart of Fig. 2 with a single vortex at the center penetrating the BEC. Figure 5 (a), a simply-connected case, is similar to Fig. 2 (a) except that it has a negative energy mode at  $m = -1$ . This mode corresponds to the typical vortex precession that is the building block for Tkachenko modes in the case of vortex lattices [20]. It is interesting to note that Fig. 5 (e), an annulus case when compared to Fig. 2 (e), does not show such additional mode even though one

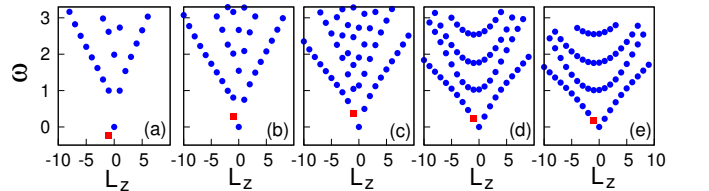


FIG. 5: (Color online)  $L_z$  vs.  $\omega$  for different  $r_0$  values for a condensate with a vortex at the center:  $r_0 = 0$  (a), 2 (b), 4 (c), 6 (d) and 7 (e). Red rectangle corresponds to a vortex precession mode at  $m = -1$ .

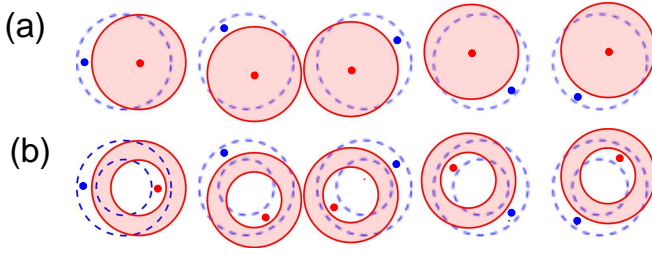


FIG. 6: (Color online) (a) Temporally successive (from left to right) snapshots of  $(0, -1)$  mode for a rotating simply-connected condensate and (b) those of  $(1, -1)$  mode for an annular condensate with perpetual current. Blue dashed circles show the positions of ground state BEC. The red dot for each plot is the vortex that gives perpetual current to the BEC while the blue dot represents the induced antivortex accompanied by the  $m = -1$  excitation.

can still make adiabatic deformation from Fig. 5 (a) to (e). We confirm that during the deformation, the vortex precession mode with a negative energy in Fig. 5 (a) adiabatically shifts to  $(0, -1)$  mode in Fig. 5 (e).

This unusual adiabatic stabilization of a vortex precession mode is made possible by the changes of the topology. As  $r_0$  increases deforming the simply-connected condensate into an annular one, the negative energy quasiparticle mode that makes the vortex state energetically unstable as a ground state acquires positive energy at  $r_0 \approx 0.8$  because of the vortex pinning by the central potential bump. Once density hole is formed in the middle of the BEC with a large enough  $r_0$  the precessing vortex behaves like the induced vortex singularities for an outer surface wave exciting the corresponding inner surface wave. This eventually forms annular density wave yielding  $(0, -1)$  mode.

On the other hand, a mode with  $(0, -1)$  in a simply-connected condensate shows center-of-mass motion that makes a clockwise circular sloshing dynamics around a small circle with the vortex sympathetically following the density maximum [Fig. 6 (a)]. Such a sympathetic mo-

tion of the vortex is a resonant behavior against the collective hydrodynamic excitation [17]. As the condensate transforms into an annular shape, this vortex motion also changes into an inner surface wave such that the nodes of inner and outer surface wave are out of phase, which corresponds to  $(1, -1)$  mode [See Fig. 6 (b)]. It is important to note that only  $m = -1$  modes can make resonant dynamics with the singly-quantized vortex at the center of a rotating simply-connected BEC. With such resonant dynamics,  $(n, -1)$  mode in a simply-connected BEC adiabatically deforms into  $(n + 1, -1)$  mode in an annular BEC. This resonant behaviour lowers the energy of the normal mode so that the  $m = -1$  mode has the lowest frequency for each family of  $n$  in a rotating annular BEC with a singly-quantized vortex at the center. This can be generalized to a rotating annular BEC with a vortex with higher winding number  $m_v > 1$  such that a mode with  $(0, -m_v)$  shows the characteristics of hydrodynamic surface excitations on the inner surface with  $m_v$  nodes while it can be adiabatically transformed from the Tkachenko mode of a vortex lattice in a simply-connected case.

In summary, our study on the Bogoiubov-de Gennes excitations of annular BEC reveals that the additional inner surface excitations are analytical continuations of collective excitations of a simply-connected condensate and that the topological aspect of the annulus forces inner surface waves associated with vortex dipoles. These aspects give rise to interesting topological phenomena such as population oscillation and new vortex nucleation process. It is further found that, with perpetual current, the inner surface excitations have distinct connection to the Tkachenko modes in a simply-connected condensate.

*Note added.* Recently, we learned of a related preprint [21].

We thank Prof. Jung Hoon Han for fruitful discussions. Y.-W.S. was supported by the NRF grant funded by the Korea government (MEST) (QMMRC, No. R11-2008-053-01002-0) and the CAC of KIAS.

- 
- [1] J. A. Sauer, M. D. Barrett and M. S. Chapman, Phys. Rev. Lett. **87**, 270401 (2001).
  - [2] S. Gupta *et al.*, Phys. Rev. Lett. **95**, 143201 (2005).
  - [3] C. Ryu *et al.*, Phys. Rev. Lett. **99**, 260401 (2007).
  - [4] A. Ramanathan *et al.*, Phys. Rev. Lett. **106**, 130401 (2011).
  - [5] A. A. Penckwitt, R. J. Ballagh and C. W. Gardiner, Phys. Rev. Lett. **89**, 260402 (2002).
  - [6] A. Aftalion and P. Mason, Phys. Rev. A **81**, 023607 (2010).
  - [7] R. Kanamoto, L. D. Carr and M. Ueda, Phys. Rev. Lett. **100**, 060401 (2008).
  - [8] F. Piazza, L. A. Collins and A. Smerzi, Phys. Rev. A **80**, 021601(R) (2009).
  - [9] R. Citro, A. Minguzzi and F. W. J. Hekking, J. Phys.: Conf. Ser. **150**, 032015 (2009).
  - [10] P. Mason and N. G. Berloff, Phys. Rev. A **79**, 043620 (2009).
  - [11] J.-P. Martikainen *et al.*, Phys. Rev. A **64**, 063602 (2001).
  - [12] T. W. Neely *et al.*, Phys. Rev. Lett. **104**, 160401 (2010).
  - [13] A. D. Jackson and G. M. Kavoulakis, Phys. Rev. A **74**, 065601 (2006).
  - [14] A. Griffin, Phys. Rev. B **53**, 9341 (1996).
  - [15] A. J. Leggett, Rev. Mod. Phys. **73**, 307 (2001).
  - [16] The time, length, energy, and angular momentum are measured in the units of  $\omega_{xy}^{-1}$ ,  $\sqrt{\hbar/M\omega_{xy}}$ ,  $\hbar\omega_{xy}$  and  $\hbar$ .
  - [17] S. J. Woo, L. O. Baksmaty, S. Choi and N. P. Bigelow, Phys. Rev. Lett. **92**, 170402 (2004).
  - [18] L. O. Baksmaty, S. J. Woo, S. Choi and N. P. Bigelow, Phys. Rev. Lett. **92**, 160405 (2004).

- [19] L. P. Pitaevskii and A. Rosch, Phys. Rev. A **55**, R853 (1997).
- [20] A. L. Fetter and A. A. Svidzinsky, J. Phys. **13**, 135 (2001).
- [21] R. Dubessy, T. Liennard, P. Pedri, and H. Perrin (2012), arXiv:1204.6183v1.